EFFECTS OF RIBLET ON FLOW STRUCTURE AROUND A NACA 0026 AIRFOIL

Z. Harun[1], A. A. Abbas[1], A. Etminan[1], B. Nugroho[2]
V. Kulandaivelu[3] and M. Khashehchi[4]

[1] The National University of Malaysia, 43600 UKM Bangi, Malaysia
[2] The University of Melbourne, Charlton, Victoria 3010, Australia
[3] The University of Utah, Salt Lake City, Utah 84112, US
[4] The University of Queensland, Brisbane St Lucia, Queensland 4072, Australia

ABSTRACT

This project focuses on the effect of riblets applied to the surface of a NACA 0026 airfoil. The airfoil with external geometry of 600 mm span, 615 mm chord and 15.6 mm thickness has been built using mostly woods and aluminum. Riblets with dimensions height h = 1 mm, pitch or spacing s = 1 mm and angle $\alpha = 0^o$ [1] using silicone rubber is attached to approximately 5% of the airfoil surface, flushed. A comparison of flow behaviour between smooth and riblet surfaces is made in moderate Reynolds numbers. Turbulence quantities are collected using hotwire anemometry. Velocity and turbulence intensities are analysed. Furthermore, a comparison using computational finite volume code, Fluent, is also performed to complement these statistics by using of κ-ε turbulent modelling. In all numerical simulations, the perpendicular mesh algorithm is used. The location of separation and reattachment points depends on the riblets arrangement and geometry. The angle of attack influences the wake region structure as well. We also study the effects of riblets towards vortex formation and its shedding around and past airfoil [3, 4].

INTRODUCTION

Originally, microstructure scale grove-like topology is observed in fast swimming sharks. These grooves and ribs are aligned with the swimming direction of these sharks [5], for simplicity, this surface is called riblets or riblet surface. Riblets dimensions are later appropriately scaled with experiments and simulations and recent studies have shown riblet surface could alter flow qualities in the near wall region [1,6] similar to pressure gradient effects [2]. More importantly riblet surface application, applied with optimized dimensions, could reduce drag force by a range up to 10% [7,8]. Paintings and coatings with microstructural riblets have been applied in aerospace and maritime applications with similar drag reduction results [9]. These are remarkable developments because of the long term economics values if drag-reducing surfaces are used in commercial transportation sector. The last citation also highlights that aerodynamic drags amount to 50% of total drag for a large passenger aircraft. The savings in fuel usage would be tremendous if these efforts could be commercialized, where riblets are applied in commercial vehicles, trucks boat and aircraft.

Riblets have been tested on airfoils, namely NACA 0012 [7,8]. In this research, we conduct the experiment with NACA 0026 airfoil. Furthermore, we provide numerical simulations to complement the experimental results and when possible, provide comparisons between the two.

EXPERIMENTAL SET UP

A purpose-built NACA 0026 airfoil has been fabricated using mostly wooden structure, polycarbonate surface, stainless steel support and aluminum end plates. The chord, c is 614 mm and the span s_p is 600 mm. The thickness, t is 15.6 mm. The chord line falls on the mean camber line, therefore this is a symmetrical airfoil. End plates are attached to the sides to minimize two-dimensionality issues. A 16 mm diameter stand, made of stainless steel is attached to one side. The riblet surface on both sides of the airfoil is applied using glue; this is shown by the black strip in Figure 1. The length of the riblet surface is 30 mm. The riblets surfaces are applied here because there is sufficient area where the effect could be experienced by the rest of the airfoil until the trailing edge.

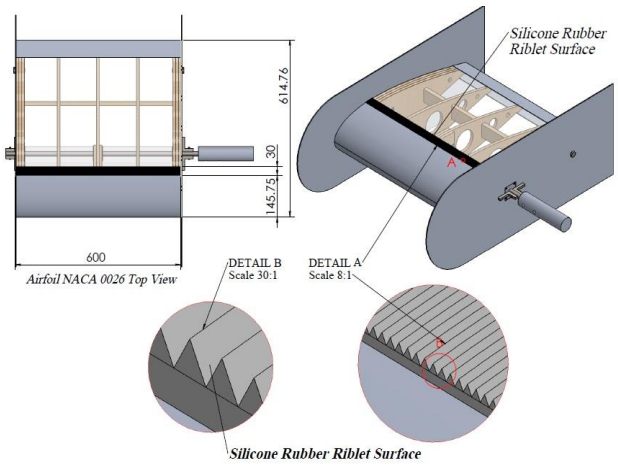

Figure 1. NACA 0026 airfoil dimension and application of riblet

The riblets are made from silicone rubber. A mould fabricated from aluminum has been machined using high precision CNC machine. Silicone rubber is applied evenly into the mould manually, however the thickness have been controlled so as to match with the triangular cavities provided on the airfoil hence riblet surface flush with the remaining airfoil surface. Prior to using silicone rubber, different riblets material such as resin-epoxy mixtures has

been tested; however their surface quality was poor. The resin-epoxy mixtures were more brittle and small particles could be found on riblets surface. For this experiment, the angle of the flow relative to the riblet direction is zero ($\alpha = 0^o$), the height, h = 1 mm and the spacing, s = 1 mm. Figure 2 shows s and h. Note that, in this figure, s appears longer than h due to the bending of the riblet surface to obtain a clear photograph.

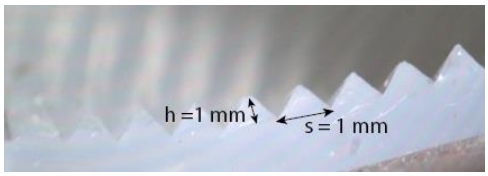

Figure 2. Silicone rubber riblet

The experiment has been conducted at the low speed wind tunnel at the Aeronautical Engineering Laboratory, Universiti Teknologi Malaysia; this wind tunnel frequently referred as UTM –LST. The UTM-LST is a closed circuit wind tunnel with 2.0 m wide, 1.5 m height and 5.5 m length test section [9]. By the use of a built-in heat exchanger as a regulator system, the temperature variation is almost negligible. Figure 3 illustrates the NACA 0026 mounted on the drag-balance system. A spanwise-vertical traverse is located approximately 1.5 m downstream. The traverse is newly built, with a ball screw pitch of 1.6 mm coupled with Vecta stepper motors model PK266 ensure a traversing resolution well below 0.1 mm in the spanwise and vertical directions. We used Velmex model VXM-3 controllers sequenced automatically with the acquisition system.

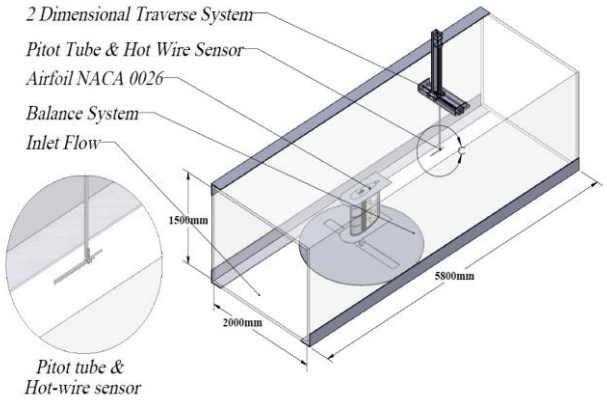

Figure 3. General arrangement of NACA 0026 airfoil in UTM-LST

The data acquisition system is the National Instrument's compactRio model NI 9074. The hotwire data is collected using module NI 9215 while all other sensors such as temperature, static pressure (pitot-tube), atmospheric pressure room humidity and dew point were collected using module NI 9215. This system allows measurement performed at very high frequency. It is important that we employ high frequency so that turbulence characteristics could be gathered [2]. The hotwire calibration was performed in-situ. Some of the information on data acquisition is described in Table 1.

Aerodynamic drag is exerted on the airfoil when wind tunnel has been started and air flow passes through it. This force is due to a combination of the shear and pressure forces acting on the surface of the airfoil. The determination of these forces is difficult since it involves the measurement of both velocity and pressure fields near the surface of the object. Drag balance system is used to directly measures the aerodynamic forces on the model.

Table 1. Experiment equipment

Equipment	**Specification**
Acquisition system	National Instrument's cRio model NI 9074
Hot-wire anemometry	Mini CTA 54T30
Sensor	Gold plated wire probes, Dantec 55P05, 5 μm, 0.8 overheat ratio.
Temperature, atmospheric pressure and room humidity sensor	Comet, model H7331
Pressure differential	LSI-Lastem model ESP024

RESULTS AND ANALYSIS

Hotwire experiment

The locations of hotwire sensor, pitot tube, two dimensional traverse system and balance measurement are shown in Figure 4. The distance of the rod of the traverse to the trailing edge is 1300 mm, and it is adjusted so that the distance between the sensor and the trailing edge to be approximately 2 c. The vertical position of the sensors is 147 mm above the centerline of the airfoil.

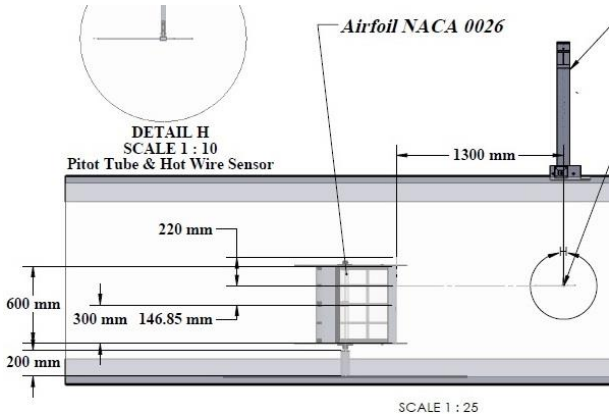

Figure 3. Location of hotwire and pitot tube during calibration and vertical and horizontal movement

The first measurement performed is the turbulence level at approximately 10 m/s where there is no airfoil in the wind tunnel.

Figure 5 shows samples of velocity fluctuations when the airfoil was not placed inside the wind tunnel (with and without the riblet surfaces). As shown in Table 2, the turbulence level is small, therefore we expect quality flows for subsequent measurements in the wind tunnel. When the

airfoil is inserted as in Figure 3 (or 4), we notice 112% increase in turbulence level.

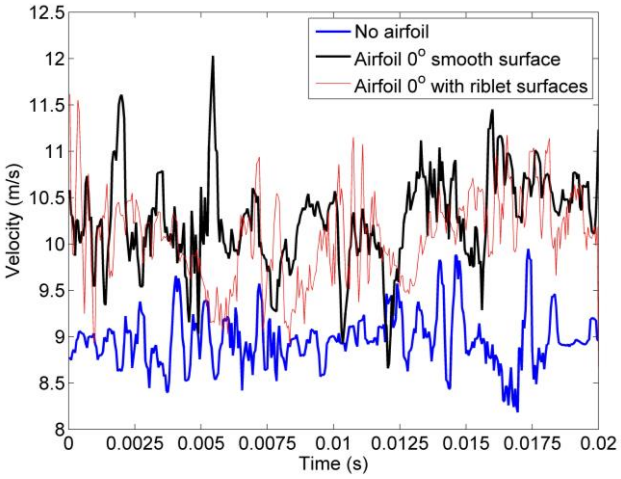

Figure 5. Sample of velocity fluctuation taken at approximately 10 m/s for different conditions

Table 2. Turbulence levels

Condition	**Turbulence levels**
No airfoil	0.4254
Airfoil with no riblet surface	0.8980
Airfoil with riblet surface on both sides	0.9480

Although there is a slight increase in turbulence level i.e. 5.6% when the riblet surface were attached to the airfoil and it is not substantial. In order to understand the turbulence levels, we analyse these flow quantities as shown in Figures 6(a) and (b).

Figure 6(a) shows the turbulence levels at 2 *c* downstream when the airfoil has no riblet surfaces. All the readings here show turbulence level well above the 0.42 level when no airfoil was placed in the wind tunnel. There is a significant fluctuation of turbulence levels observed in turbulence profile as shown in this figure although sufficiently long acquisition time has been allowed (60 *s* at f_s = 20 kHz). However, it is quite clear that the maximum turbulence levels occurs only within -0.5*t* < *thickness* < 0.5*t*. We could not move the sensors much further away from the centerline t = 0 (dash-dot vertical lines in Figures 6(a) and (b)), nonetheless it is expected that turbulence level reduces gradually with distance from centerline and reaches 0.42 level at distance 3 *t* from the centerline.

Figure 6(b) describes velocity profiles at 2 *c* downstream from the trailing edge. The mean velocity is slightly above the targeted velocity of 10 m/s. Similarly the velocity only decreases within -0.5*t* < *thickness* < 0.5*t* where the maximum decrease is within the centerline itself at approximately 6.5% from bulk velocity of approximately 10.8 m/s.

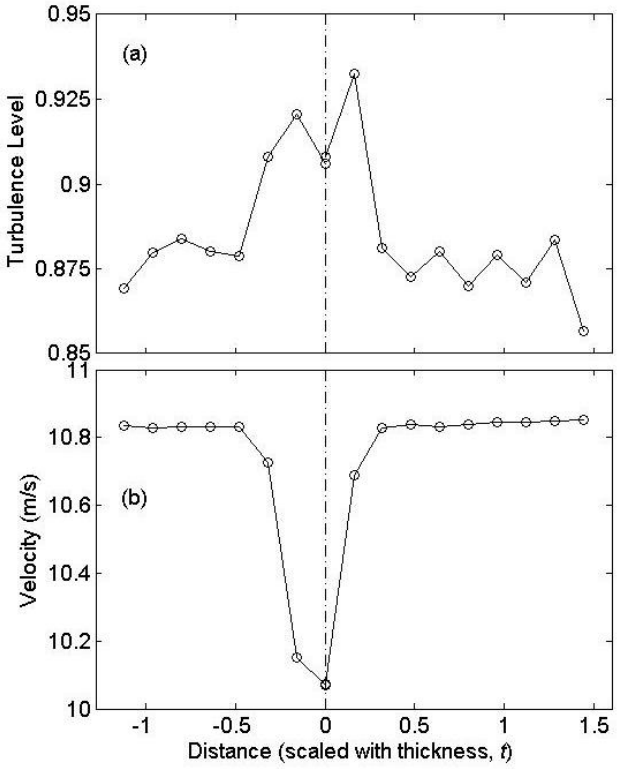

Figure 6. Flow quantities at 2 *c* downstream, (a) Turbulence and (b) Velocity profiles across thickness. The dashed-dot lines are centrelines.

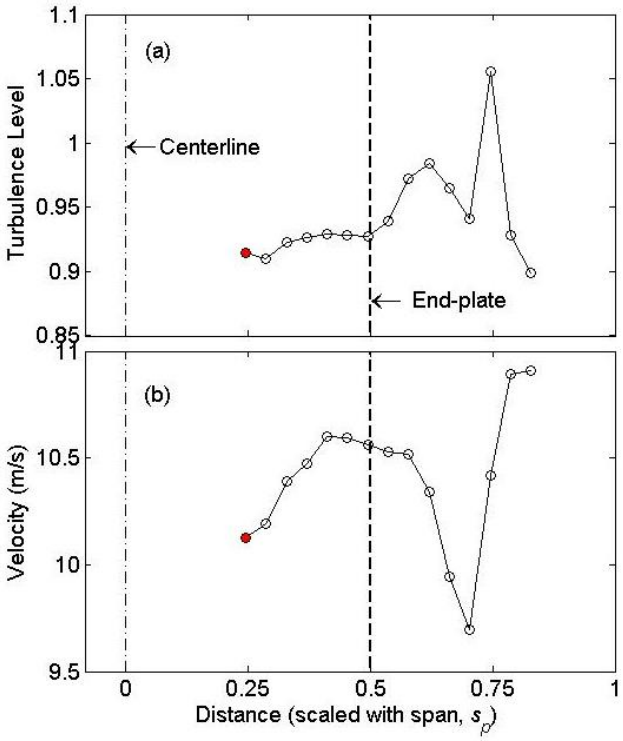

Figure 7. Flow quantities at 2 *c* downstream, (a) Turbulence and (b) Velocity profiles across span s_p

Figure 7(a) demonstrates the turbulence levels at 2 *c* downstream when the airfoil has no riblet surfaces. This set of data was also measured in 60 *s* at f_s = 20 kHz for each point. The distance is scaled with the span s_p. The dash-dot

line is the centerline of the airfoil across the span. The measurement starts at a quarter of the whole span towards the end-plate. The starting point of measurement is the filled circle in the figure. The end-plate is marked with the thicker dashed line. Turbulence levels are observed to be constant across $0.25 < s_p < 0.5$ i.e. within the end plate. However, some fluctuations are observed beyond the end plate. It should be noted that the location of the starting point in this figure is the same as for the data which lies on the centerline in Figure 6(a). The two figures suggest that turbulence level is approximately constant across the span with fluctuation within 1.5% (within the end plate regions). However turbulence levels fluctuate more across the thickness at approximately 6%. Because of these small fluctuations, drag and balance measurement systems allow us to calculate the data with more accuracy.

Likewise, Figure 7(b) shows the velocity profile at 2 *c* downstream. Velocity increases towards the end-plate before abruptly decreased beyond the end plate. Note that velocity magnitude is minimum at the centreline of the thickness when moving across the thickness.

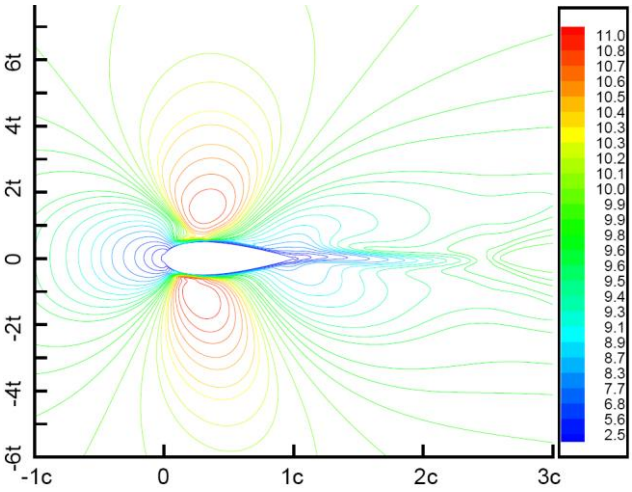

(a)

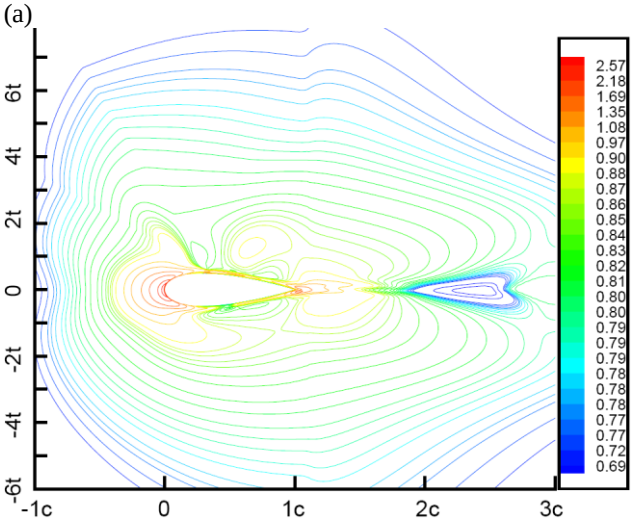

(b)

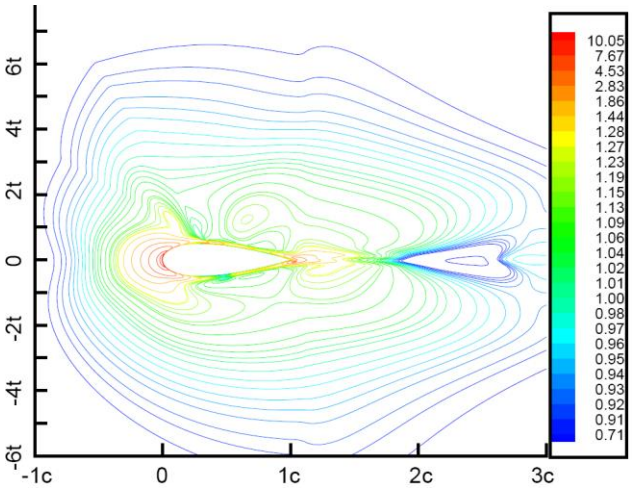

(c)

Figure 8. Contour of (a) X-velocity, (b) turbulent intensities and (c) turbulent kinetic energy around the airfoil on left-hand side and riblet surface on right-hand side

Flow structure in the vicinity of the airfoil

To complement our highly constrained experiments, we performed simulations. The simulations results are meant to provide further understanding of velocity, turbulent intensities and energy distributions. The contours of X-velocity, turbulent intensities and turbulent kinetic energy respectively around the airfoil are shown in Figure 8. Since it is to obtain flow properties from simulations, we have increased the horizontal and vertical range of study. For example, Figure 8(a) shows a range of -1 *c* < chord < 3 *c*, much wider than the experimental range of a line at location 3 *c* (or 2 *c* downstream from the trailing edge of the airfoil as mentioned in Figure 2). The stagnation point in the frontal side of the airfoil could be observed. Generally the velocity on top (positive t direction) and bottom of the air foil is symmetric. Velocity is minimum just at the start of the trailing edge and recovers almost homogeneously to within 9.6 - 9.9 m/s (within 0.3 m/s band) at 3 *c*. This however does not match with experimental results at the same location as shown in Figure 6 (b) which shows non-homogeneous pattern within 10.1 – 10.8 m/s (0.7 m/s) with the minimum clearly shown within the low velocity core along downstream from the trailing edge. Figure 8(b) shows turbulent intensities contours. There seems to be an area where turbulence intensities are minimum i.e. at approximately 2.5 *c*. There seems to be disagreements with the experimental results as in Figure 6(a).

As expected, turbulence kinetic energy in Figure 8(c) is similar to turbulence intensities distribution. Turbulence intensities and kinetic energy are high near it surface due to the friction and near-wall shear effects. At the trailing edge, there seems to be an area where turbulence kinetic energy peaks i.e. at location approximately 0.3 *c*. This is due to a overlapping of vortices from both top and bottom side of the airfoil.

Drag and balance experiment and numerical results

Determination of drag force has been considered as the ultimate goal during experiments and simulations. The drag and balance experiment was conducted for angle of attack AoA 0^o until 30^o with an increment of 5^o. The drag and balance equipment employed by UTM-LST has accuracy of 0.04% [10].

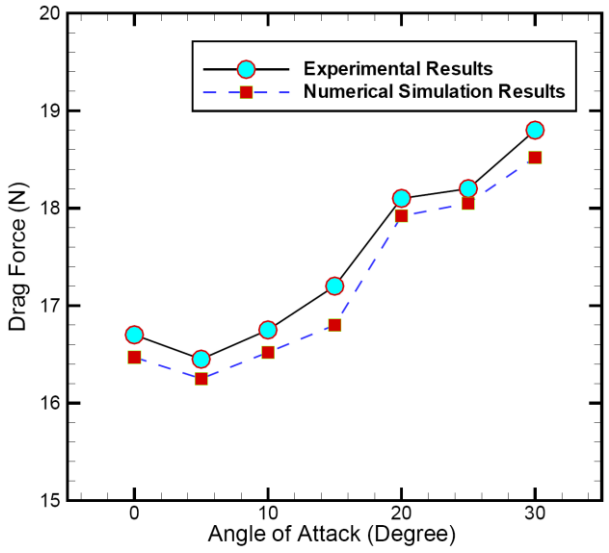

(a)

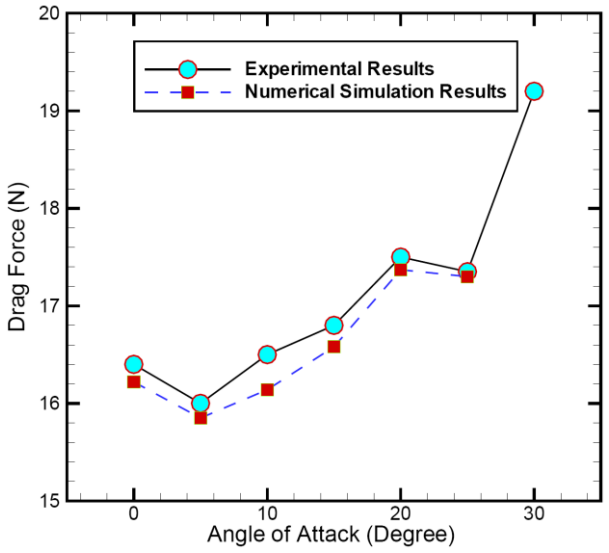

(b)

Figure 9. Variation of the drag force versus the selected angle of attacks for, (a) smooth surface and (b) riblet surface

Although the data available comprise of spanwise and lift elements, and all three moments, we will present only the axial data i.e. direct force onto the airfoil. Figure 8 shows total drag experienced in comparison with numerical simulations by the entire airfoil (with end plates) for both clean surface (circle) and 30 mm riblets surface applied as in Figure 1. Riblet surfaces reduce the drag experienced by the surface. Even though the reduction of total drag from the two cases presented here is only approximately 1.5%, there is a clear trend except of the largest AoA = 30^o. At AoA = 30^o, turbulence intensities measured for airfoil with riblets is higher than that measured with clean surface. The exception here might be attributable to the fluctuation arising from increased turbulence i.e. the effect generated from AoA is greater than that of surface. The data presented here is within the expectation [6,7,8,11].

It can be observed that numerical results are in good agreement with experimental outputs. The small deviation between them is related to the experimental instruments and numerical fault such as rounding up or down and etc.

CONCLUSION

The hotwire anemometry and drag and balance experiment performed using NACA 0026 reveal that a small portion of riblet applied at the front end of airfoil surface could enhance turbulence. In general, turbulence causes total drag to decrease. Simulation results confirm this too and additionally provide more information on the overall flow structure around the airfoil. This study is still ongoing as turbulence measurements shall be performed directly on the airfoil surface for better understanding of flow qualities.

We would like to express our gratitude for the financial supports provided by UKM research grant FRGS/1/2013/TK01/UKM/03/1 and the staff at the Aeronautical Engineering Laboratory, UTM Skudai, Malaysia.

NOMENCLATURE

α	angle between flow direction and riblet alignment
AoA	angle of attack
f_s	sampling frequency
c	airfoil chord (from airfoil definition)
h	riblet height
s	riblet spacing
s_p	airfoil span (from airfoil definition)
t	airfoil thickness (from airfoil definition)

REFERENCES

(1) Nugroho, B., Hutchins, N., Monty, J.P. (2013): "Large-Scale Spanwise Periodicity in a Turbulent Boundary Layer Induced by Highly Ordered and Directional Surface Roughness". *Int. J. of Heat and Fluid Flows*, Vol. 41, pp. 90–102.

(2) Harun, Z., Monty, J. P., Mathis, R., and Marusic, I., (2013): "Pressure Gradient Effects on the Large-Scale Structure of Turbulent Boundary Layers". *J. Fluid Mech.* Vol. 715, pp. 477-498.

(3) Etminan, A., Jafarizadeh, H., Moosavi, M. and Akramian, K., (2012): "Determination of Flow Characteristics and Turbulent Heat Transfer in a Ribbed Roughened Square Duct, Part 1: Turbulence Models", *Applied Mechanics and Materials Journal*, Vol. 110-116, pp. 2359-2363.

(4) Etminan, A., Jafarizadeh, H., Moosavi, M., and Akramian, K. (2012): "Determination of Flow Characteristics and Turbulent Heat Transfer in a Ribbed Roughened Square Duct, Part 2: Numerical

Simulations". *Applied Mechanics and Materials Journal*, Vol. 110-116, pp. 2364-2369.

(5) Dean, B., and Bhushan B., (2012): "Shark-skin surfaces for fluid-drag reduction in turbulent flow: a review". *Phil. Trans. R. Soc. Lond. A.*, Vol. 368, pp. 4775 - 4806.

(6) Garcia-Mayoral, R., Jimenez, J., (2011): "Drag reduction by riblets". *Phil. Trans. R. Soc. Lond. A.*, Vol. 369, pp. 1412–1427.

(7) Sareen, A., Deters, R.W., Henry, S.P., and Selig M.S. (2011): "Drag Reduction Using Riblet Film Applied to Airfoils for Wind Turbines" *AIAA Jan. meeting, Orlando, FL*, doc. 558.

(8) Viswanath, P.R. (2002): "Aircraft viscous drag reduction using riblets", *Prog. In Aero. Sciences*, Vol . 38, pp. 571–600.

(9) Stenzel, V., Wilke, Y. and Hage, W. (2011) "Drag-reducing paints for the reduction of fuel consumption in aviation and shipping", *Progress in Organic Coatings*, Vol. 70. pp. 224–229.

(10) Alias, M.N., and Mansor, S. (2013): "Measuring Aerodynamic Characteristics Using High Performance Low Speed Wind Tunnel at Universiti Teknologi Malaysia". *Applied Mechanical Eng.* Vol. 3 (1), 1000132.

(11) Devinant, Ph., Laverne, T., and Hureau, J. (2002): "Experimental Study of Wind-Turbine Airfoil Aerodynamics in High Turbulence", *J. of Wind Eng. and Industrial Aerodynamics*, Vol. 90, pp. 689-7